THE PERMEABILITY OF RANDOM DISCONTINUOUS CARBON FIBRE PREFORMS

Andreas Endruweit, Lee T. Harper, Thomas A. Turner, Nicholas A. Warrior and Andrew C. Long

School of Mechanical, Materials and Manufacturing Engineering, University of Nottingham, University Park, Nottingham, NG7 2RD, U.K.
andreas.endruweit@nottingham.ac.uk

ABSTRACT

During liquid injection of chopped random preforms, increasingly uneven flow fronts develop with increasing fibre length and filament count. The results of injection experiments suggest that the permeability of the preforms decreases with increasing level of bundle fragmentation (i.e. filamentisation). At typical fibre volume fractions for DCFP preforms (20 % to 40 %), the preform permeability generally tends to be in a similar order of magnitude to that of conventional fibrous reinforcements at the respective typical fibre volume fractions. Whilst for fibres with a high propensity for intrinsic bundle splitting, the preform permeability increases continuously with increasing fibre length because of increasing level of residual bundling, no such trend can be identified for fibres with a low propensity for bundle splitting. Fibre characteristics such as applied sizing and tow cross-sectional shapes affect the intrinsic filamentisation behaviour and may dominate the preform permeability. Qualitatively, the numerical results obtained from a stochastic permeability model agree with the experimental observations. The simulated filling patterns are useful for identifying promising injection strategies, and the predicted global permeabilities may allow comparison of different preforms.

1. INTRODUCTION

Directed carbon fibre preforming (DCFP) is an automated spray-deposition process for the manufacture of chopped random fibre preforms for Liquid Composite Moulding (LCM). Fibres are typically ejected from automatically operated mechanical chopping heads using a combination of linear motion induced fibre conveying and additional high speed air. A polymeric powder binder is employed to allow stable preforms to be made. Fibres, together with the binder, are sprayed onto a perforated tool, and air is evacuated from the underside to retain the sprayed fibres. A matched perforated upper tool is used to compact the preform to a defined thickness while hot air is cycled through the perforations to activate the binder.

Typical applications are in the automotive industry, where DCFP components offer the potential for 40 % to 60 % weight reduction compared to steel [1]. Cost savings over more conventional carbon fibre processing technologies are significant and may become more so with the introduction of low-cost, high filament count tows (> 24K). The preform permeability governs the resin impregnation process and thus the production cycle time, as well as the properties of the finished component. The in-plane permeability is unknown for DCFP because the preform architecture differs significantly from that of textile fabrics and other more conventional random filament mats. In addition, the tows tend to fragment during processing, creating a distribution of bundle sizes, which further increases the complexity of the architecture. Published experimental and theoretical permeabilites of these fibrous reinforcements are therefore unavailable. Due to the stochastic distribution of fibre bundles in DCFP preforms, the porosity and permeability are inherently non-uniform. In LCM processes, this results in irregular resin flow behaviour at the macroscopic scale. Because of the randomness of the resin flow, outcomes of the preform impregnation are hard to predict, which

negatively affects control of the component quality and process optimisation. This study aims to characterise the in-plane permeability of chopped carbon fibre preforms, which are currently used for semi-structural panels with relatively low wall thickness of around 2 mm. The effects of material parameters such as fibre length and virgin tow size on the preform impregnation are presented. A stochastic permeability model is developed and implemented in resin injection simulations.

2. EXPERIMENTAL PERMEABILITY CHARACTERISATION

2.1 Materials

The DCFP preforms used in the injection experiments for permeability measurement were produced from carbon fibre bundles with filament counts c_f of 3K, 6K, 12K and 24K (Toho Tenax Europe GmbH), with identical filament diameters of 7 μm. The sizing employed was epoxy on the bundles with lower c_f (3K, 6K) and polyurethane on the bundles with higher c_f (12K, 24K). Two variants of the 24K material ("E" and "J") were used, which have identical specifications but an undisclosed difference in winding during manufacture. Available fibre lengths l for preform production, determined by the chopper head, are integer divisions of 115 mm. The chopper head elevation above the tool surface was Δz = 300 mm. The distribution of the chopped fibre bundles throughout the preform is determined by the spray path pattern followed by the robot, on which the chopper head is mounted.

During DCFP processing, carbon fibres tend to cohere in a tow due to the fibre surface treatment. There is an increased natural tendency for the tow to fragment when cut shorter, hence filament count is proportional to fibre length. This intrinsic splitting is dependent on the level and type of sizing agent applied to the fibre. For the 24K tows, the "E" fibre has a high tendency to fragment when chopped to short lengths compared with the "J" fibre. Further filamentisation of the tow (Figure 1) can be induced using high velocity air perpendicular to the direction of fibre travel after chopping.

During fibre deposition, 6 % by weight of thermoset powder binder (Reichhold Pretex 110) was added to the fibres, resulting in an approximate effective fibre density ρ = 1.73×10^3 kg/m^3. The preforms were compacted at 0.2 bar and cured for 5 min at 150 °C to activate the binder.

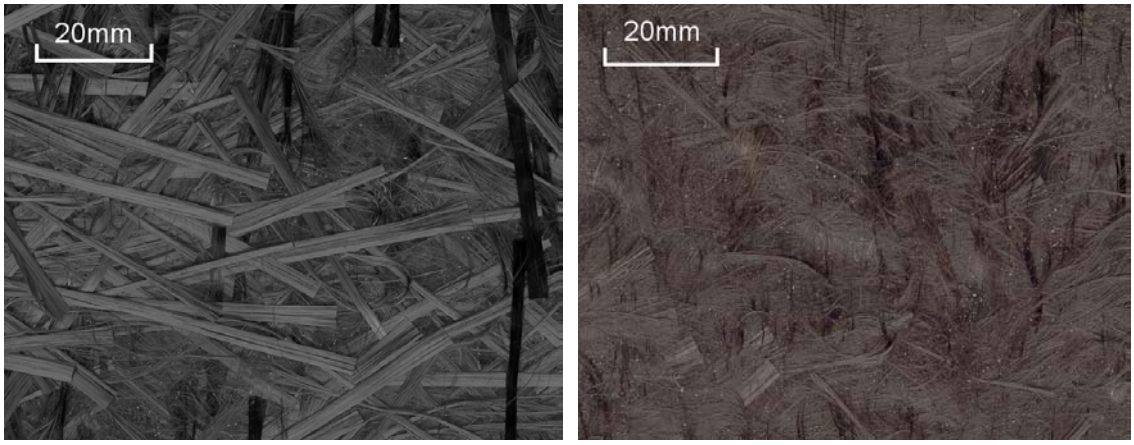

Figure 1: Comparison of the preform fibre architecture for a virgin 24K tow (left) and a highly filamentised 24K tow (right).

The chopped fibre preforms are generally structured on multiple scales. The micro-scale structure refers to the distribution of filaments and inter-filament voids within the

fibre bundles. The meso-scale structure characterises the arrangement of fibre bundles and inter-bundle voids, and the macro-scale structure describes the distribution of fibre bundles over the component dimensions. For increasing levels of filamentisation of the fibre bundles, the meso-scale structure converges to the micro-scale structure.

2.2 Results

The unsaturated in-plane permeability of chopped random fibre preforms was determined in radial [2,3] (typically four repeats) and uni-directional [4] (typically six repeats) injection experiments at a given injection pressure. While the permeability values obtained from radial and uni-directional injection experiments are consistent for conventional textile fabrics, they may differ for DCFP preforms. This observation is related to the experimental techniques employed: If the preform is highly heterogeneous, i.e. the flow front is not circular or elliptical, the basic assumption for application of the data reduction scheme is not met. Therefore, the radial injection experiments lead to a misrepresentation of the global preform permeability. Visual observations indicate that the deviation of the flow front shape from a perfect circle or ellipse becomes increasingly significant with increasing fibre length and virgin tow size, and with decreasing levels of fragmentation. Therefore, uni-directional flow experiments have been performed for these preforms. Whilst these experiments also showed irregular flow front propagation, the flow tends to remain macroscopically uni-directional, even for non-uniform preforms.

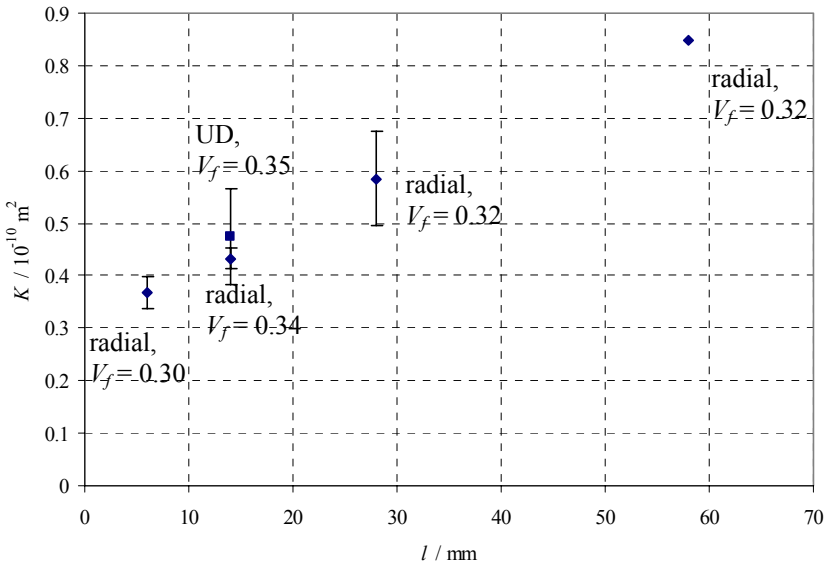

Figure 2: Permeability K as a function of the fibre length l at maximum induced filamentisation (24K yarns), measured in radial and uni-directional (UD) injection experiments; "E" fibres; the actual average global fibre volume fraction V_f for each data point is given.

In addition, the observed difference between the permeability values obtained from radial and uni-directional injection experiments decreases with decreasing fibre bundle size, because the different impregnation mechanisms related to the preform micro- and meso-structure converge at high levels of filamentisation. For preforms comprising highly fragmented 24K tows, permeability values measured in both radial and uni-directional injection experiments appear to be in close agreement. The permeability increases continuously with increasing fibre length (Figure 2). This trend may be

explained by the decreasing propensity for bundle splitting with increasing fibre length (for "E" type fibres [5]). The resulting greater effective bundle diameter is expected to cause higher permeability values and increased local non-uniformity, which agrees with the qualitative observation that the flow front shape tends to be more uneven for longer fibre segments. The effects of fibre length and bundle splitting on the permeability cannot be separated here.

However, as the level of preform homogeneity decreases, i.e. for high filament count bundles, the results from the uni-directional injection experiments appear to be significantly lower than those of the radial injections (Table 1). In this case, it was also observed that the results generally show high variations, such that no clear trend can be identified for the effect of increasing length. This can be explained by the generally low propensity of the "J" type bundles to splitting.

Identification of the influence of the filament count on the preform permeability (Figure 3) is difficult, since other fibre characteristics may vary as well. An increase in permeability with increasing c_f as suggested by the difference between 24K tows at high and low levels of filamentisation cannot be observed. Different types of sizing used on the fibres, and different tow cross-sectional shapes may affect the filamentisation behaviour [5]. As shown in Table 1, two different 24K tows ("E" and "J") show significantly different permeabilities measured in uni-directional experiments.

Table 1: Global fibre volume fraction V_f and permeability K for preforms from "J" or "E" fibres with l = 58 mm, c_f = 24K, at no induced filamentisation, measured in radial or uni-directional (UD) injection experiments.

	"J", radial	"E", UD	"J", UD
V_f	0.33 ± 0.02	0.36 ± 0.02	0.32 ± 0.01
K / 10^{-10} m^2	5.240 ± 2.567 (± 49 %)	0.603 ± 0.067 (± 11 %)	2.153 ± 0.939 (± 44 %)

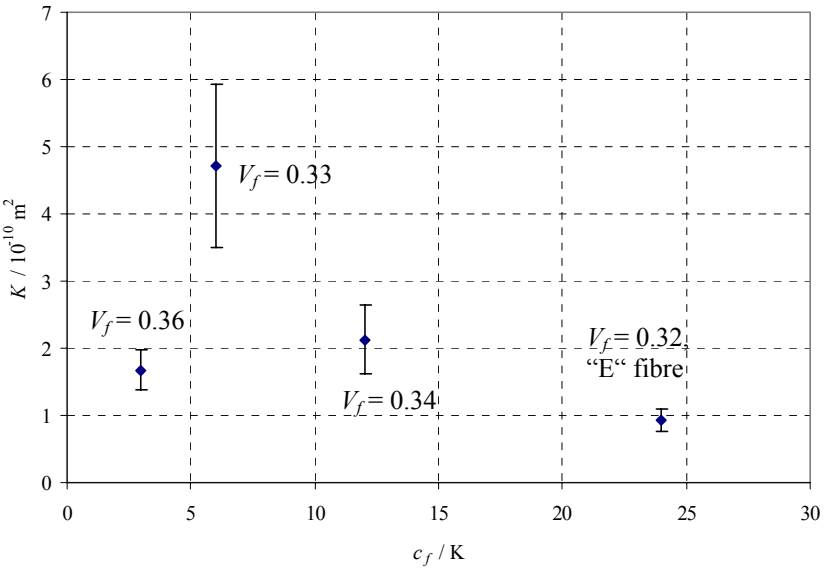

Figure 3: Isotropic permeability K as a function of the filament count c_f of the virgin fibres at no induced filamentisation (l = 28 mm), measured in uni-directional injection experiments; the actual average global fibre volume fraction V_f for each data point is given.

Quantitatively, the permeability of the DCFP preforms is typically in the order of 10^{-11} m^2 to 10^{-10} m^2, depending on the fibre volume fraction (Table 2) and degree of bundle splitting. This implies that the preform permeability generally tends to be in a similar order of magnitude as that of conventional fibrous reinforcements at the respective typical fibre volume fractions. Regarding the expected mould fill times, the preforms are suitable for use in industrial component manufacture.

Table 2: Isotropic permeability K as a function of the global fibre volume fraction V_f at a filament count c_f = 24K at no induced filamentisation (l = 28 mm), measured in uni-directional injection experiments.

V_f	0.32 ± 0.01	0.40 ± 0.03	0.48 ± 0.05
K / 10^{-10} m^2	2.114 ± 0.736	0.743 ± 0.366	0.698 ± 0.244

3. PREFORM MODELLING

A simulation tool has been developed to describe the influence of both fibre and process related parameters on the geometrical structure of DCFP preforms. The fibre bundles are characterised by the filament count c_f, the length l, the linear density λ (a function of the filament count) and the width w. While the actual bundle cross-sections typically show characteristics of elliptical, lenticular and almost rectangular shapes, here they are assumed to be flat (rectangular) and are characterised by a "bundle superficial density"

$$S_0 = \frac{\lambda}{w} \quad . \tag{1}$$

The distribution of fibre bundles throughout the preform depends on the robot sweep pattern, speed and tool elevation. These parameters determine the ranges of three random numbers for each deposited bundle, the polar co-ordinates of the bundle centroid and an angle describing the bundle orientation [1].

The preform is discretised along the co-ordinate x- and y-directions into a grid of $n_x \times n_y$ square cells with edge length L. Once the simulation of the spray deposition process is complete, the number of fibre bundles, N, and the orientations of the fibre bundles, α_i, are determined at the centroid of each cell (Figure 4). The local fibre volume fraction V_f is determined from N according to

$$V_f = \frac{N S_0}{h \rho} \quad , \tag{2}$$

where S_0 is defined according to Eq. (1), ρ is the density of the fibre material and h is the cavity height. It is assumed that the filaments are distributed evenly across the cavity height. The principal permeability values k_1 and k_2 of an individual fibre bundle in a cell with fibre volume fraction V_f are calculated based on the equations derived by Gebart [6],

$$k_1 = \frac{R_f^2}{4 c_1} \frac{(1 - V_f)^3}{V_f^2} \quad \text{and} \quad k_2 = c_2 \left(\sqrt{\frac{V_{f\max}}{V_f}} - 1 \right)^{5/2} R_f^2 \quad , \tag{3}$$

where R_f is the filament radius and c_1, c_2 and V_{fmax} are geometric constants (Table 3).

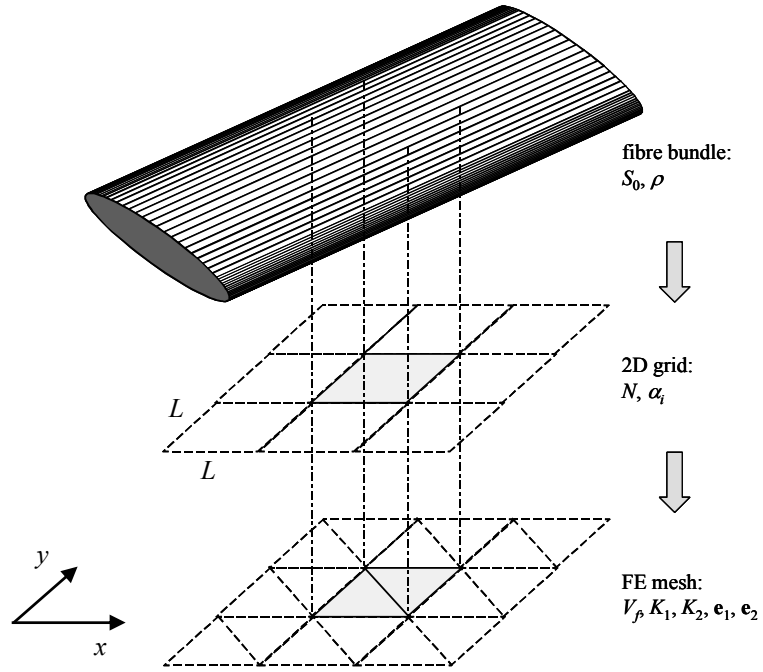

Figure 4: Derivation of the material parameters for a finite element flow simulation from the fibre bundle properties S_0 and ρ and the geometrical preform characteristics N and α_i.

Table 3: Density of fibre material ρ, filament radius R_f, geometric constants c_1, c_2 and V_{fmax} (for square fibre packing) and cavity height h used to calculate fibre volume fraction and permeability according to Eqs. (2) and (3); viscosity of the injected fluid η, pressure difference between injection gate and flow front Δp are also given.

ρ / kg/m^3	R_f / mm	c_1	c_2	V_{fmax}	h / mm	η / Pa·s	Δp / 10^5 Pa
1750	7×10^{-3}	1.78	0.40	0.785	2	0.1	1

N may be zero in some instances. In this case, k_1 and k_2 according to Eq. (3) have infinite values, and the bundle permeability is replaced by the equivalent channel permeability

$$k_c = \frac{h^2}{12} \quad , \tag{4}$$

as discussed by Ni et al. [7].
The angle α_0, which describes the orientation of the principal material axis of the stack of N bundles, and the principal stack permeabilities K_1 and K_2 can be derived from thickness-weighted averaging of the bundle permeabilities. Vectors $\mathbf{e}_1$ and $\mathbf{e}_2$ for the orientations of the principal permeabilites K_1 and K_2 are then calculated from the angle α_0. The parameters V_f, K_1, K_2, $\mathbf{e}_1$ and $\mathbf{e}_2$ calculated for each cell are assigned to the corresponding finite elements on a triangular mesh, as illustrated in Figure 4. The equations describing the flow of a viscous liquid through a porous medium, considering

conservation of the fluid mass, can then be solved based on a non-conforming finite element method [8], implemented in the PAM-RTM software (ESI Group).

4. RESIN INJECTION SIMULATION

Uni-directional resin injection at constant injection pressure was simulated for a configuration with a linear injection gate along one of the short edges of the rectangular preform. The dimensions of the preform were L_x = 280 mm and L_y = 110 mm. For fibre bundles with different filament count c_f, the bundle superficial density S_0 was determined according to Eq. (1) from the linear density λ and the measured typical bundle width w. The values of S_0 and the parameters listed in Table 3 were substituted in Eqs. (2) and (3) to determinate the fibre volume fraction and the permeability of the fibre bundles. It was ensured that the width w of the fibre bundles was not significantly smaller than L, in order to prevent the local permeability variations to be underestimated by cell-wise averaging.

Based on the injection simulations, the global preform permeability can be determined according to

$$K = -\frac{x_{ff}^2 \, \Phi \, \eta}{2 \Delta p \, t_{ff}} \quad , \tag{5}$$

where Δp is the pressure difference between injection gate and flow front, η is the viscosity of the injected fluid (Table 3), x_{ff} is the flow front position, t_{ff} is the time for the flow front to reach x_{ff}, and

$$\Phi = 1 - V_f \tag{6}$$

is the porosity of the preform. Here, V_f refers to the global fibre volume fraction which can be determined by substituting the preform-averaged number of bundles per cell, N, in Eq. (2). The time t_{ff} is determined from the pressure increase at a virtual pressure sensor at a position x_{ff} = 250 mm, y = 55 mm.

The average value and the standard deviation of K can be determined from statistical evaluation of the results from a series of simulations. The average value represents the global permeability, while the standard deviation (or the coefficient of variation) reflects the unevenness of the flow front, which is caused by the local preform non-uniformity. The standard deviation allows calculation of an envelope for the most likely flow front position at a given injection time.

The influence of the parameters filament count c_f, length l and target superficial density S_t for parallel spray paths in x-direction (spray path offset Δy = 30 mm, tool elevation Δz = 300 mm) on the permeability was determined based on a L9 (3^3) Taguchi design. Evaluation of the results in Table 4 indicates that the global preform permeability decreases with increasing superficial density (i.e. the average fibre volume fraction) and is independent of the filament count and the fibre bundle length. Increasing filament count and fibre bundle length, however, results in increasing unevenness of the flow front and thus of the observed coefficient of variation of the permeability. The coefficient of variation increases with increasing superficial density because fluid exchange along the flow front is reduced and thus its unevenness is increased.

Table 4: Global permeability K (mean value, standard deviation and coefficient of variation, based on five repeats) determined from injection simulations at different values of the parameters filament count c_f, bundle length l, preform target superficial density S_t; for the number of bundles per cell, N, and the local fibre volume fraction for each cell, V_f, mean value, standard deviation and coefficient of variation were averaged for each series.

c_f / 10^3	l / mm	S_t / kg/m^2	N	V_f	K / 10^{-11} m^2
6	28	0.70	4.08 ± 2.07 (± 51 %)	0.19 ± 0.10 (± 53 %)	4.73 ± 0.23 (± 5 %)
6	57	1.05	6.10 ± 2.44 (± 40 %)	0.29 ± 0.12 (± 41 %)	1.36 ± 0.04 (± 3 %)
6	115	1.40	8.01 ± 2.76 (± 34 %)	0.38 ± 0.13 (± 34 %)	0.49 ± 0.04 (± 8 %)
12	28	1.05	6.11 ± 2.55 (± 42 %)	0.30 ± 0.13 (± 43 %)	1.39 ± 0.05 (± 3 %)
12	57	1.40	8.08 ± 2.73 (± 34 %)	0.40 ± 0.14 (± 35 %)	0.44 ± 0.03 (± 8 %)
12	115	0.70	4.02 ± 1.89 (± 47 %)	0.20 ± 0.09 (± 45 %)	4.28 ± 0.29 (± 7 %)
24	28	1.40	8.14 ± 2.80 (± 34 %)	0.40 ± 0.14 (± 35 %)	0.58 ± 0.07 (± 12 %)
24	57	0.70	3.98 ± 1.80 (± 45 %)	0.19 ± 0.09 (± 47 %)	5.05 ± 0.45 (± 9 %)
24	115	1.05	6.13 ± 2.30 (± 37 %)	0.30 ± 0.11 (± 37 %)	1.29 ± 0.13 (± 10 %)

At constant preform superficial density, variation of the preform processing parameters (fibre spray path offset Δy, spray tool elevation Δz, and spray path pattern) affects the fibre bundle distribution and thus the flow front patterns. Two different spray patterns were considered. Either 100 % of the total fibre mass was deposited in lines parallel to the x-direction, or 50 % was deposited in lines parallel to the x-direction and 50 % in lines parallel to the y-direction with an offset Δy in both directions (orthogonal). Examples for the distributions of fibre bundles and the corresponding results of injection simulations are shown in Figure 5.

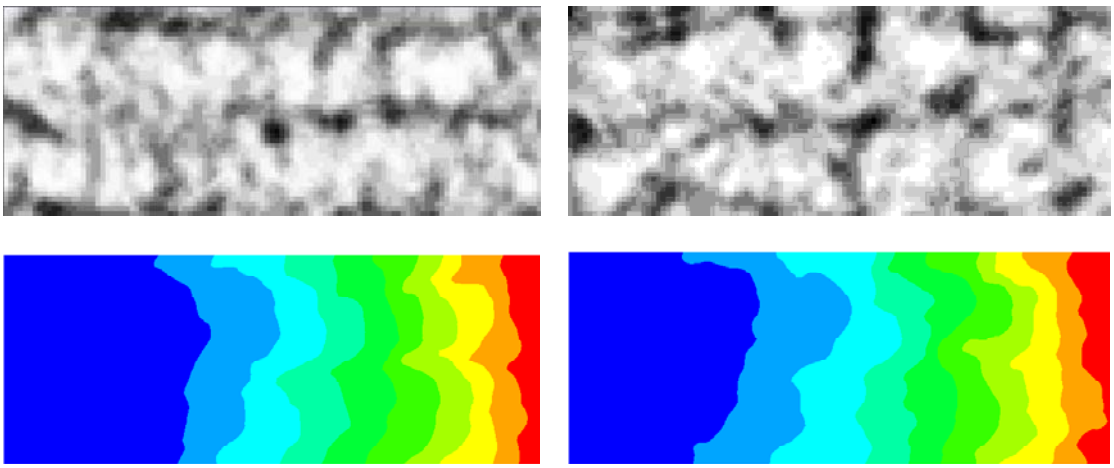

Parallel, Δy = 50 mm, Δz = 100 mm Orthogonal, Δy = 50 mm, Δz = 100 mm

Figure 5: Top: Examples for distributions of fibre bundles (greyscale indicates N). Bottom: Corresponding flow front patterns for injection from left to right.

Preforms with parallel spray paths at relatively wide spacing show uneven flow fronts, propagating faster in the zones with relatively low fibre density than in the zones with

high density. For the preforms with orthogonal spray paths, the same effect can be observed, but the flow front is repeatedly levelled by the low permeability zones perpendicular to the main flow direction. Different combinations of the processing parameters have different effects on the mould fill times. For preforms with parallel spray paths along the main flow direction, uneven flow fronts are correlated to short fill times. For preforms with orthogonal spray paths, on the other hand, short fill times occur for evenly distributed fibres.

5. CONCLUSIONS

The permeability values of DCFP preforms obtained from radial and uni-directional injection experiments may differ. The significance of this effect decreases with decreasing fibre bundle size, because of different impregnation mechanisms related to the preform micro- and meso-structure. In general, uni-directional injection experiments are more suitable to obtain reliable permeability values for this type of preform. Visual observation indicates that with increasing fibre length and increasing filament count, increasingly uneven flow fronts develop during the injection process. This has implications for industrial applications, since increasing variability results in increased scrap rates and problems in tool design.

The permeability of preforms with a high degree of fragmentation is significantly lower than that of preforms with low fragmentation at identical fibre lengths. At typical fibre volume fractions for DCFP preforms, the preform permeability generally tends to be in a similar order of magnitude as that of conventional fibrous reinforcements at the respective typical fibre volume fractions. Whilst highly fragmented tows have been previously shown to improve the mechanical performance, they significantly impact on the manufacturing performance, causing a significant increase in fill time due to the reduced permeability. For fibres with a high propensity for intrinsic bundle splitting, the preform permeability increases continuously with increasing fibre length because of increasing level of residual bundling. At high filament count and low propensity for bundle splitting, no trend can be identified. Identification of the influence of the filament count on the preform permeability is difficult, since other fibre characteristics, such as applied sizing and tow cross-sectional shapes, which may affect the intrinsic filamentisation behaviour, may vary as well.

The qualitative observation that flow fronts were increasingly uneven with increasing filament count and increasing fibre length, agrees with the numerical results obtained from a stochastic permeability model. To achieve better quantitative agreement between the predictions and the experimentally determined permeabilities, the multi-scale structure of the preforms, i.e. bundling of filaments and the effective filament count in the bundles, which is affected by intrinsic bundle splitting, would need to be accounted for in the simulations. However, the simulated filling patterns may help to identify promising injection strategies, and the predicted global permeabilities may allow comparison of different preforms.

ACKNOWLEDGEMENTS

This work was funded by the Engineering and Physical Science Research Council (EPSRC), as part of Platform Grant GR/T18578/01, and the Nottingham Innovative Manufacturing Research Centre. The authors wish to thank Toho Tenax Europe GmbH for supply of carbon fibres. ESI Group are also thanked for the use of the PAM-RTM software.

REFERENCES

1- Harper, L.T., Turner, T.A., Warrior, N.A., Dahl, J.S. and Rudd, C.D., "Characterisation of random carbon fibre composites from a directed fibre preforming process: Analysis of microstructural parameters", *Composites Part A*, 2006; 37: 2136-2147.

2- Weitzenböck, J.R., Shenoi, R.A., Wilson, P.A., "Radial flow permeability measurement. Part A: Theory", *Composites Part A*, 1999; 30: 781-796.

3- Weitzenböck, J.R., Shenoi, R.A., Wilson, P.A., "Radial flow permeability measurement. Part B: Application", *Composites Part A*, 1999; 30: 797-813.

4- Ferland, P., Guittard, D., Trochu, F., "Concurrent methods for permeability measurement in resin transfer molding", *Polymer Composites*, 1996; 17: 149-158.

5- Harper, L.T., Turner, T.A., Warrior, N.A. and Rudd, C.D., "Characterisation of random carbon fibre composites from a directed fibre preforming process: The effect of tow filamentisation", *Composites Part A*, 2007; 38: 755-770.

6- Gebart, B.R., "Permeability of Unidirectional Reinforcements for RTM", *Journal of Composite Materials*, 1992; 26: 1100-1133.

7- Ni, J., Zhao, Y., Lee, L.J., Nakamura, S., "Analysis of two-regional flow in liquid composite molding", *Polymer Composites*, 1997; 18: 254-269.

8- Trochu, F., Gauvin, R., Gao, D.M., "Numerical analysis of the Resin Transfer Molding process by the finite element method", *Advances in Polymer Technology*, 1993; 12(4): 329-342.